# Simulation and Optimization of Diesel Quality and Yield from Waste Tire Pyrolysis Using Aspen Plus

**Mohammad Gharib Blouck [1] - Ali Sadeghikia [2] - Vahid chegeni [3] - Farid Azizi [3] - Mojtaba Azizi [4,5,*]**

[1] Faculty of Management and Accounting, Yadegar Imam Khomeini(RAH) Branch, Islamic Azad University, Tehran. Iran
[2] School of Chemical Engineering, College of Engineering, University of Tehran, Tehran, Iran
[3] Department of Computer Engineering, Khorramabad Branch, Islamic Azad University, Khorramabad, Iran
[4] Organic and Nano Group (ONG), Faculty of Chemistry, Iran University of Science and Technology (IUST), PO Box 16846-13114, Tehran, Iran
[5] Faculty of Chemistry and Chemical Engineering, Malek Ashtar University of Technology, P.O. Box 16765-3454, Tehran, Iran
* Corresponding author E-mail: azizi.m_58@yahoo.com

**ABSTRACT**

*This study focuses on the simulation and optimization of the pyrolysis process of waste tires using Aspen Plus software. The primary objectives were to enhance the quality and production rate of the extracted diesel while minimizing the number of distillation trays to reduce capital investment costs [1][2]. Initial kinetic data and simulation parameters were derived from existing literature. Although the quality of the produced diesel met some standards, challenges arose in achieving optimal characteristics [3]. Specifically, attempts to balance density and distillation range resulted in trade-offs, leading to a focus on maximizing the distillation range [4]. The findings indicate that while the optimization of diesel quality was partially successful, further adjustments are necessary to achieve the desired standards [2]. This research contributes to the understanding of waste tire pyrolysis and offers insights for future improvements in the process.*

***Keywords:*** *Pyrolysis, Waste tires, Diesel, Simulation, Optimization, Aspen Plus*

## 1. *INTRODUCTION*

*The rapid growth of the automotive industry and transportation sector has led to a significant increase in waste tire accumulation, posing serious environmental challenges [5]. When discarded improperly, waste tires can contaminate soil, water, and air, resulting in pollution and health hazards. Traditional disposal methods such as landfilling and open burning have been prohibited in many countries, necessitating the development of more effective and sustainable solutions [5]. Among various disposal techniques, pyrolysis has emerged as one of the most promising methods for waste tire management [5].*

*Pyrolysis is a thermochemical conversion process that decomposes waste tires into valuable products under high temperatures in the absence of oxygen, typically in an inert atmosphere such as nitrogen [6]. This process not only addresses environmental concerns but also offers potential for energy recovery, producing bio-oil, bio-char, and syn-gas. The pyrolysis of waste tires has become a focus of research due to its ability to generate useful products while mitigating pollution [7]. One of the attractive aspects of this process is the production of carbon black, a material widely used in industrial applications, which can be extracted from waste tires through pyrolysis. This pyrolytic carbon black (CBp) has shown promise in performing some functions of traditional carbon black, either directly or after certain purification processes [8].*

*The pyrolysis process involves complex heat transfer and chemical reactions. As the feedstock is heated, it undergoes thermal decomposition, resulting in the production of solid, liquid, and gaseous products. The*

*distribution and quality of these products depend on various factors, including temperature, heating rate, and particle size of the feedstock. The pyrolysis process typically occurs over a temperature range of 400°C to 700°C [7][6], where the rubber components break down into a complex mixture of hydrocarbons [8]. Studies have shown that the pyrolysis behavior can vary significantly depending on the type of tire, with truck tires generally being easier to pyrolyze than other types [6].*

*To optimize the pyrolysis process and predict its outcomes, researchers have developed various models and simulation techniques. These models typically incorporate kinetic, heat transfer, and hydrodynamic sub-models to provide a comprehensive understanding of reactor behavior. Advanced simulation models, which include kinetic rate-based reaction mechanisms and equilibrium separation models, have been developed to assess the technical performance of the process. Computer simulations and software tools, such Aspen Plus, have been employed to analyze and optimize pyrolysis reactors [6]. By combining experimental data with theoretical models, researchers can gain valuable insights into the pyrolysis process and work towards improving its efficiency and economic viability [8].*

*Kinetic modeling plays a crucial role in understanding the pyrolysis reaction and determining important parameters such as activation energy and frequency factors. Various kinetic models have been employed to analyze the pyrolysis process, revealing that the reaction typically follows a multistep mechanism. The insights gained from these kinetic studies are essential for the development and optimization of waste tire pyrolysis processes on an industrial scale. Moreover, vacuum conditions during pyrolysis have been found to significantly impact the process, allowing for easier product condensation and control of composition, which enhances the quality of the resulting diesel [7].*

*Furthermore, techno-economic analyses have been conducted to evaluate the feasibility of implementing pyrolysis technology at various scales [5]. These studies have revealed that the economic viability of waste tire pyrolysis plants is strongly dependent on processing capacity, with larger-scale operations generally offering better profitability and shorter investment payback periods. As the world continues to seek sustainable solutions for waste management and energy production, optimizing waste tire pyrolysis processes becomes increasingly important [5].*

*This article aims to provide an optimum condition for waste tire pyrolysis modeling and simulation, explore the impact of process parameters on product yields and composition, and discuss the economic considerations for implementing pyrolysis technology. By synthesizing these insights, we hope to contribute to ongoing efforts to address the global challenge of waste tire management while simultaneously recovering valuable resources and enhancing energy security.*

## *2. METHODOLOGY*

*The optimization of diesel quality and yield from waste tire pyrolysis is a complex process that requires a thorough understanding of both the chemical transformations involved and the operational parameters that influence product characteristics. In this study, we employed advanced simulation software, specifically Aspen Plus, to model the pyrolysis process and optimize the extraction of diesel cut from pyrolysis oil.*

*The methodology outlined in this section is designed to systematically approach the challenges associated with waste tire pyrolysis, focusing on enhancing the quality of the diesel produced while maximizing yield. The initial phase involved the reconstruction of existing simulations from relevant literature, which served as a foundation for our research. This step was crucial in establishing a reliable baseline for comparison and validation of our results.*

*Following the reconstruction, we conducted a rigorous validation process to ensure that the simulation outcomes aligned with experimental data, thereby confirming the accuracy of our model. This validation was essential for establishing credibility in our findings and ensuring that subsequent modifications to the model would yield meaningful results.*

*To enhance the simulation, we incorporated two distillation columns into the model, enabling the separation of the diesel fraction from the pyrolysis oil. This addition presented new challenges, particularly in meeting the stringent requirements for diesel quality, including density and distillation range. Throughout the optimization process, we faced the inherent trade-offs between achieving optimal density and maintaining the desired distillation range, which necessitated a careful balancing act.*

*The subsequent sections will detail the specific steps taken in the methodology, including the challenges encountered, the optimization strategies employed, and the evaluation of the results. By meticulously documenting these processes, we aim to provide a comprehensive overview of our approach to optimizing diesel quality and yield from waste tire pyrolysis, contributing valuable insights to the field of renewable energy and waste management.*

## *3. RECONSTRUCTION OF PREVIOUS SIMULATIONS*

*In this phase of the methodology, we focused on reconstructing simulations based on existing studies in the field of waste tire pyrolysis. To begin, we reviewed several key articles that provided insights into the pyrolysis of waste tires, specifically examining their methodologies, parameters, and results. We identified critical variables such as temperature, heating rates, and residence times that were commonly used in these studies. The parameters selected for our reconstruction were aligned with those reported in the literature to ensure consistency and comparability.*

*As a guideline, Cao et al [6] and Ismail et al [7] works is followed and developed. These models could be defined in 3 stages:*

### 3.1. Preparing The Feed

*The feed of plant is large size particles of waste tire (1100-1600 mm) that contains metal wires. This size distribution was chosen because of the assumption that truck tires would be used in the process. In the first Stage this Stream enters a Crusher (EQ1) to reduce particle size to 8-15 mm. The Particle Size Distribution (PSD) of feed and other streams are shown in* Appendix A. *Other conditions of streams are shown in* Appendix B. *Also, input and results of each equipment are shown in* Appendix C.

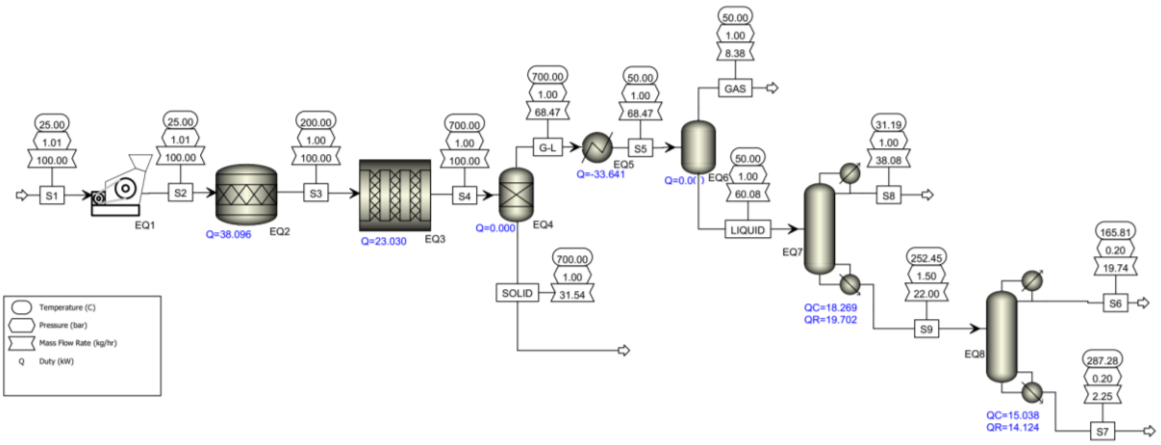


**Fig. 1.** *Process Flow Sheet in Aspen Plus*

### 3.2. Pyrolysis Reaction

*The pyrolysis reaction stage was illustrated in the flowsheet as a combination of a stoichiometric reactor, a plug flow reactor, and a 2-phase Separator. The non-conventional solid feed elements were transformed into their conventional essential elements by the preset stoichiometric reactor (EQ2), which operated at temperatures ranging from 400 to 700 °C under 100 kPa pressure. The products exiting the stoichiometric reactor were primarily in vapor phase, except for char black and metal ash.*

*Subsequently, the Plug reactor (EQ3), which included a reaction kinetic model for converting waste tire into liquid, solid, and vapor, was modeled. Temperature variations from 400 to 700 °C were employed to simulate pyrolysis reactions using the selected flow rate. Additionally, the reactor dimensions used in the simulation had a diameter of 0.15 m and a length of 1.7 m for the production of oil and gas products, in accordance with the specified kinetics in* Appendix *D based on Ismail et al. [7]*

### 3.3. Primary Products Separation

*To Separating Main Products (Gas, Oil, Solid) 2 Separators and one ooler are considered. In the first Separator (EQ4) Solid part of products will achieved that contain Metal, Ash and char. Then the Gas-Liquid stream enters the cooler (EQ5) to cool down to 40 ℃. The cooled stream enters second separator (EQ6) and Gas and Liquid products will exit from it.*

### 3.4. Separation and Purification of Limonene

*Ismail et al [7] focused on design an optimum process for separation and purification of Limonene as a valuable product. But in this study, design an optimum process condition to produce diesel is aimed. So, our route will be getting far about references from this point.*

## *4. VALIDATION OF SIMULATION RESULTS*

*Before adding new equipments and routes, we need to ensure the reliability and accuracy of the model in this step. The validation of simulation results is a crucial step of the model developing for optimizing diesel quality and yield from waste tire pyrolysis. In this section, we detail the methodologies employed to compare the outputs of our simulations with experimental data from the literature, thereby confirming the validity of our model.*

*To initiate the validation process, we first established a set of criteria based on key performance indicators that are commonly reported in studies of waste tire pyrolysis. These indicators included Pyrolysis yields and C7-C15 Weight fractions.*

*We then conducted a series of simulation runs using the validated model, generating output data that reflected the performance of the pyrolysis process under various operating conditions. The results obtained from these simulations were systematically compared to the experimental data sourced from the literature. This comparison involved both qualitative and quantitative analyses [9].*

*Compared simulation results with experimental data of Pyrolysis yields, is shown in Table 1. According to this, It can be seen that the amount of solid formed in the simulation data is almost constant and does not change with changes in pyrolysis temperature. This is because the definition of waste tire solid in Aspen Plus is Nonconventional and the pyrolysis process is simulated on this basis. Therefore, changes in reaction temperature and consequently in reaction kinetics will have very subtle changes in the amount of solid. So temperature changes show their effect more on the production of gas and liquid from pyrolysis.*

*As expected, with increasing pyrolysis temperature, thermal breakdown reactions in liquid compounds increase and as a result the amount of final liquid decreases and the amount of gas increases. This is observed in both experimental and simulation data.*

*It should be noted that the simulated pyrolysis gas and liquid values in Table 1 are reported after passing through the cooler (EQ5) and cooling to 25 ℃ (Ambient Temperature).*

**Table 1**. *Pyrolysis yields (wt.%) of simulated results and experimental data [10]*

| Temperator (℃) | Solid | | Liquid | | Gas | |
|---|---|---|---|---|---|---|
| | Experimental | Simulated | Experimental | Simulated | Experimental | Simulated |
| **300** | 87.6 | 32.10 | 4.8 | 62.71 | 7.6 | 5.21 |
| **400** | 55.9 | 32.25 | 24.8 | 62.03 | 19.3 | 5.86 |
| **500** | 44.8 | 32.14 | 38.0 | 61.54 | 17.2 | 6.33 |
| **600** | 44.2 | 31.92 | 38.2 | 61.18 | 17.6 | 6.92 |
| **700** | 43.7 | 31.54 | 38.5 | 61.06 | 17.8 | 7.41 |

*Then, C7-C15 Weight fractions of simulation and experimental works is shown in Figure 2. We can see that The values of both simulations are very close to each other and this is observed at all pyrolysis temperatures. Also, the difference between the values of both simulations can be justified with the experimental values. In addition, the reason for the small changes of the simulation bars with temperature is similar to that explained for Table 1.*

*This figure shows that the simulation results are acceptable in terms of the pyrolysis principle and reaction kinetics and the simulation of the current research can be extended to the next stages.*

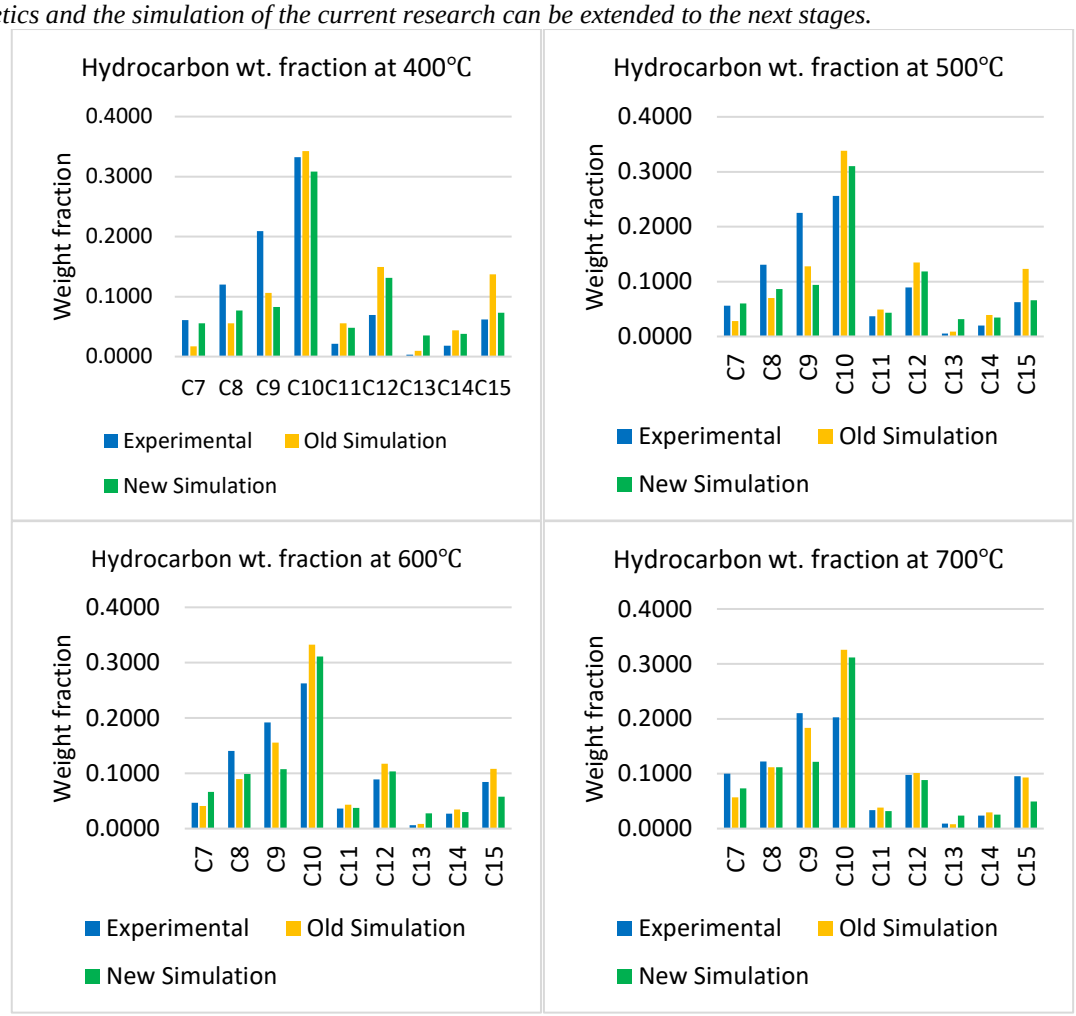


**Fig. 2.** *C7-C15 Weight fractions plot for simulated result and experimental data in 4 Reactor Temperature [10]*

*Throughout this validation process, we encountered some discrepancies between our simulation results and the experimental data. In particular, variations in product yields and specific quality parameters were noted. These discrepancies prompted us to revisit certain assumptions made during the simulation setup, such as feedstock characteristics and reaction kinetics. By adjusting these parameters and re-running the simulations, we were able to enhance the model's accuracy and better align the outputs with the experimental findings.*

*The successful validation of our simulation results not only confirmed the reliability of our model but also provided a solid foundation for the subsequent phases of our research. With a validated simulation in place, we were well-equipped to proceed with the integration of distillation columns and the optimization of diesel yield and quality, ensuring that our findings would contribute meaningfully to the ongoing discourse in waste tire pyrolysis and renewable energy production.*

## *5. ADDITION OF DISTILLATION COLUMNS*

*In this phase of the methodology, we focused on enhancing the simulation model by incorporating two distillation columns to facilitate the separation of the diesel fraction from the pyrolysis oil. The objective was*

*to optimize the extraction process and improve the quality of the diesel produced, aligning it with industry standards.*

### 5.1. Design and Configuration of Distillation Columns

*The design of the distillation columns was based on the specific requirements for separating the diesel fraction from the complex mixture of hydrocarbons present in the pyrolysis oil. We selected a two-column configuration: the first column (EQ7) was designed for separation of light components, while the second column (EQ8) was intended for separation of residue of the diesel product.*

*In the simulation software (Aspen Plus), we defined the operational parameters for both columns as an initial estimation, including the number of theoretical stage ,reflux ratio and condensor and reboiler pressure. The result of this columns is used for optimization stage of design.*

### 5.2. Integration into the Simulation Model

*Once the design parameters were established, the distillation columns were integrated into the existing pyrolysis simulation model. This integration required careful consideration of the flow rates, temperature profiles, and pressure conditions to ensure seamless operation between the pyrolysis reactor and the distillation units.*

*The simulation was run to assess the performance of the distillation columns in separating the diesel fraction. Key outputs included the composition of the distillate and residue streams, as well as critical quality parameters such as density, viscosity, and boiling point range of the diesel product.*

## *6. CHALLENGES ENCOUNTERED*

*The integration of distillation columns into the simulation model presented several challenges that required careful consideration and strategic problem-solving. These challenges primarily revolved around achieving the desired quality of the diesel product while optimizing the overall performance of the pyrolysis process. In this section, we outline the key challenges encountered during this phase of the methodology and the strategies employed to address them.*

### 6.1. Optimization of Density vs. Distillation Range

*One of the most significant challenges was the conflicting requirements for optimizing density and maintaining an acceptable distillation range for the diesel product. As we adjusted the operational parameters to achieve an optimal density-an essential quality characteristic for diesel fuel-we noticed that the distillation range often deviated from the desired specifications. Conversely, attempts to optimize the distillation range led to suboptimal density values, which could compromise the fuel quality.*

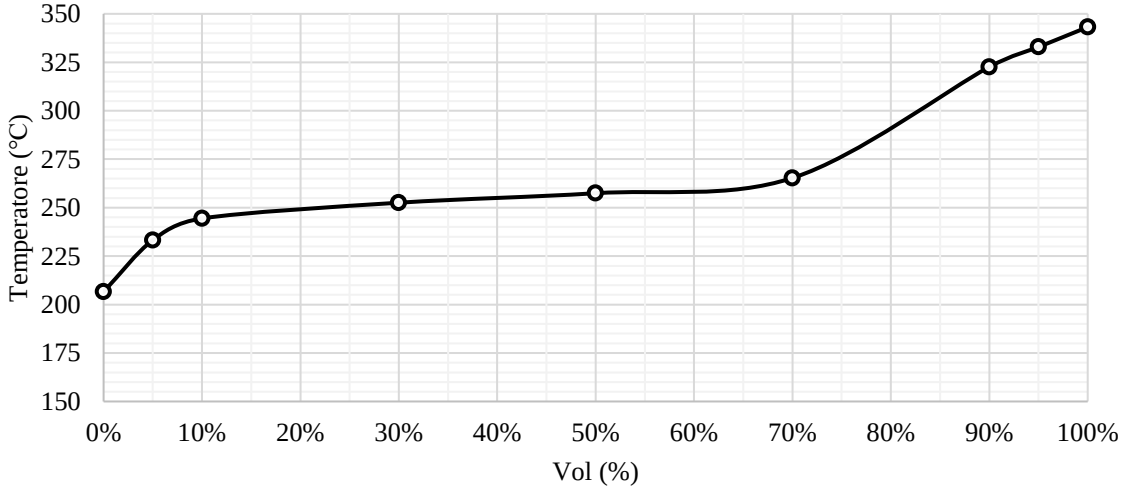


**Fig. 3.** *Distilation Range Plot **(ASTM D86)** of Produced Diesel*

**Table 2.** *Comparing Primary results of simulation with **BS EN 590** standard*

| BS EN 590 Check list | | | | | |
|---|---|---|---|---|---|
| **Property** | **Unit** | **Limits** | | **Our Data** | **Penalty (%)** |
| | | **Min.** | **Max.** | | |
| Flash point | °C | 55 | - | 96.91 | 0 |
| Carbon residue g(on 10 % distillation residue) | % (m/m) | - | 0.3 | 0 | 0 |
| Ash content | % (m/m) | - | 0.01 | 0 | 0 |
| Water content | % (m/m) | - | 0.02 | 0 | 0 |
| Viscosity at 40 °C | mm2/s | 2 | 4.5 | 2.657 | 0 |
| (V/V) recovered at 250 °C | % | - | 65 | 50 % at 257.45 °C | 0 |
| (V/V) recovered at 350°C | % | 85 | - | 100 % at 343.16 °C | 0 |
| 95 % (V/V) recovered at | °C | - | 360 | 332.88 °C | 0 |
| Cetane number | - | 51.0 | - | **17.93** | **64.84** |
| Cetane index | - | 46.0 | - | **23.27** | **49.41** |
| Density at 15 °C | kg/m3 | 820.0 | 845.0 | **963.77** | **14.05** |
| Sulfur content | mg/kg | - | 10 | 0 | 0 |

**Table 3.** *Comparing Primary results of simulation with **ASTM D975** standard*

| ASTM D975 Check list | | | | | |
|---|---|---|---|---|---|
| **Property** | **Unit** | **Limits** | | **Our Data** | **Penalty (%)** |
| | | **min** | **max** | | |
| Flash Point | °C | 52 | - | 96.91 | 0 |
| Water and Sediment | Vol % | - | 0.05 | 0 | 0 |
| Distillation Temperature at 90 % percent volume recovered | °C | 282 | 338 | 322.6 | 0 |
| Kinematic Viscosityat 40 °C | mm2/S | 1.9 | 4.1 | 2.657 | 0 |
| Ash | mass % | - | 0.01 | 0 | 0 |
| Sulfur Content | ppm | - | 15 | 0 | 0 |
| Cetane index | - | 40 | - | **23.27** | **41.83** |

*To address this issue, we conducted a thorough analysis of the relationship between these two parameters. This involved running a series of simulations to evaluate how changes in reflux ratio, feed temperature, and pressure affected both density and distillation range. Through this iterative process, we identified specific operational conditions that would allow for a more balanced approach, but the trade-offs remained a persistent challenge.*

### 6.2. Maintaining Product Quality Standards

*Another challenge was ensuring that the final diesel product met industry standards for quality. This included not only density and distillation range but also other critical parameters such as viscosity and Cetane Index. The complexity of the pyrolysis oil composition, which contains a wide variety of hydrocarbons, added to the difficulty of achieving these standards (such as **ASTM D975** and **BS EN 590**).*

*As we can see in Tables 2 and 3, All parameters are within standard limits, except for the cetane number, cetane index, and density. This is due to the trade-off between distillation range and cetane number. Because in the Base-Case study, which was assumed to be the only desired parameter of distillation range, the cetane*

*index reached an undesirable value of 16.57, which was very disappointing. However, by reducing the sensitivity to distillation range, the cetane number and index improved.*

*Another frustrating issue is density. Figure 4 and 5 shows what densities the Pyrolysis oil and Final Product components have ,respectively. Noting that these figures are shown for components with a mass fraction greater than 0.5%, we can see that most of participant components in these streams have Specific Gravity greater than 0.9, even in Primery Pyrolisys Oil. So obviously, the Specific Gravity of Final Products can never reach 0.85 just by simple and routine separation scenario. Therefore, with the present explanatory conditions and considering the lowest cost (capital and operating), the most optimal operating conditions have been calculated.*

## *7. OPTIMIZATION PROCESS*

*The optimization process was a critical phase of the methodology aimed at enhancing both the quality and yield of diesel produced from waste tire pyrolysis. This section outlines the systematic approach taken to optimize the operational parameters of the pyrolysis and distillation processes, focusing on achieving the desired product specifications while addressing the challenges identified in previous sections.*

### 7.1. Identification of Key variables and Constrants

*To initiate the optimization process, we first identified the key operational variables that significantly influence the quality and yield of the diesel product. Also to ensure that the answers do not deviate from reasonableness, constraints of each variable have been defined. These variables and constraints included:*

a. *Pyrolisys Reactor Temperature ($T_R$):*
*The most important key and influential variable in optimizing this process is the reactor temperature, which determines the conversion and rate of the liquid product.*
   - $300 \leq T_R \leq 700$

b. *Cooler Temperature ($T_C$):*
*The outlet temperature from the cooler determines the amount of gas and liquid products, as well as their compositions.*
   - $40 \leq T_C \leq 100$

c. *Recovery of heavy key component in First Column ($H_1$)*
   - $0.00001 \leq H_1 \leq 0.002$

d. *Recovery of heavy key component in Second Column ($H_2$)*
   - $0.01 \leq H_2 \leq 0.1$

e. *Recovery of light key component in First Column ($L_1$)*
   - $0.97 \leq L_1 \leq 0.99$

f. *Recovery of light key component in Second Column ($L_2$)*
   - $0.999 \leq L_2 \leq 0.9999$

g. *Molar Reflux Ratio in First Column ($R_1$)*
   - $1 \leq R_1 \leq 5$

h. *Molar Reflux Ratio in Second Column ($R_2$)*
   - $1 \leq R_2 \leq 5$

i. *Condenser Pressure in First Column ($P_{C,1}$)*
   - $0.2 \leq P_{C,1} \leq 2$

j. *Condenser Pressure in Second Column ($P_{C,2}$)*
   - $0.2 \leq P_{C,2} \leq 2$

k. *Reboiler Pressure in First Column ($P_{R,1}$)*
   - $0.2 \leq P_{R,1} \leq 2$

l. *Reboiler Pressure in Second Column ($P_{R,2}$)*
   - $0.2 \leq P_{R,2} \leq 2$

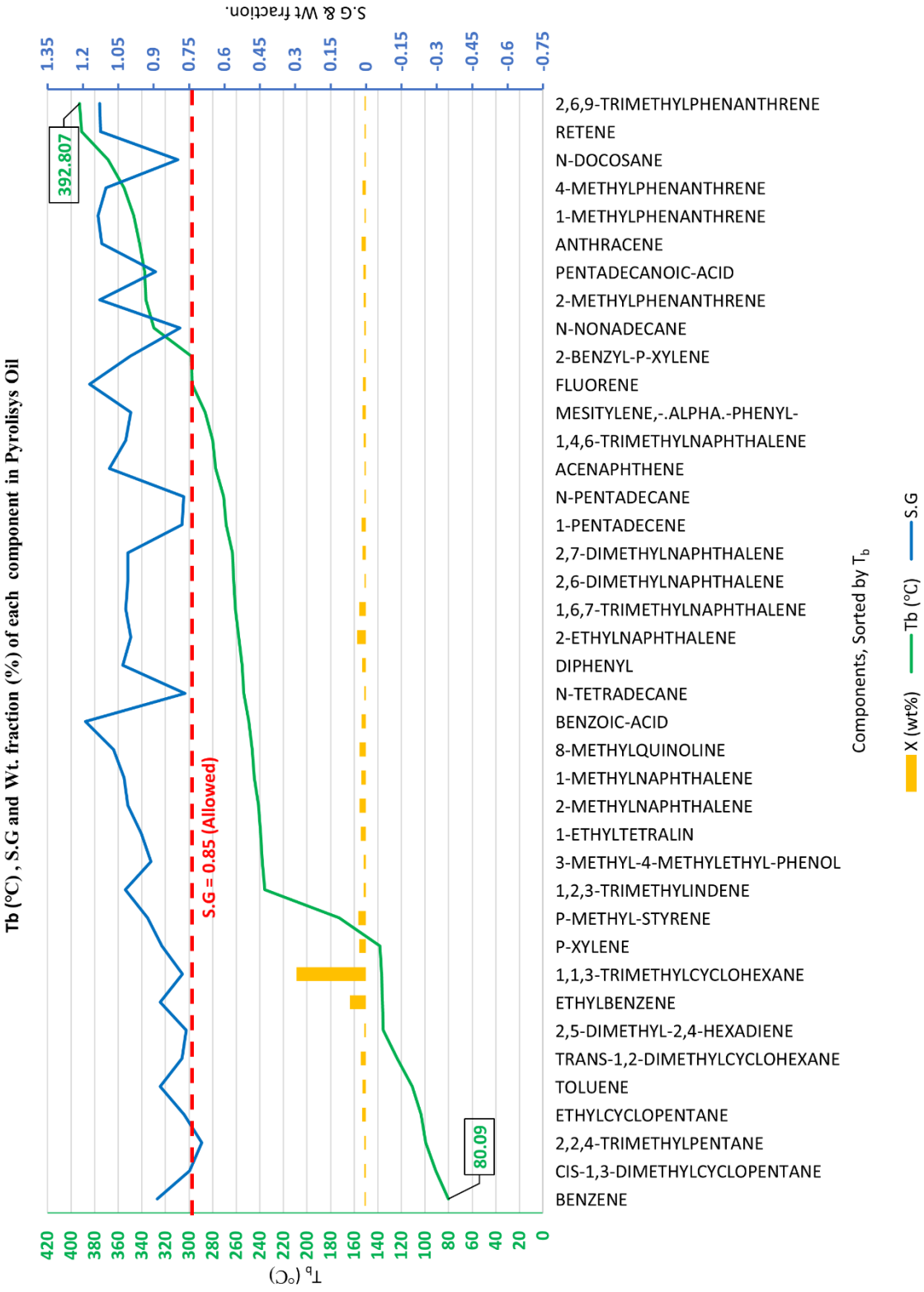


**Fig. 4.** *Components of pyrolisys Diesel and their dencity*

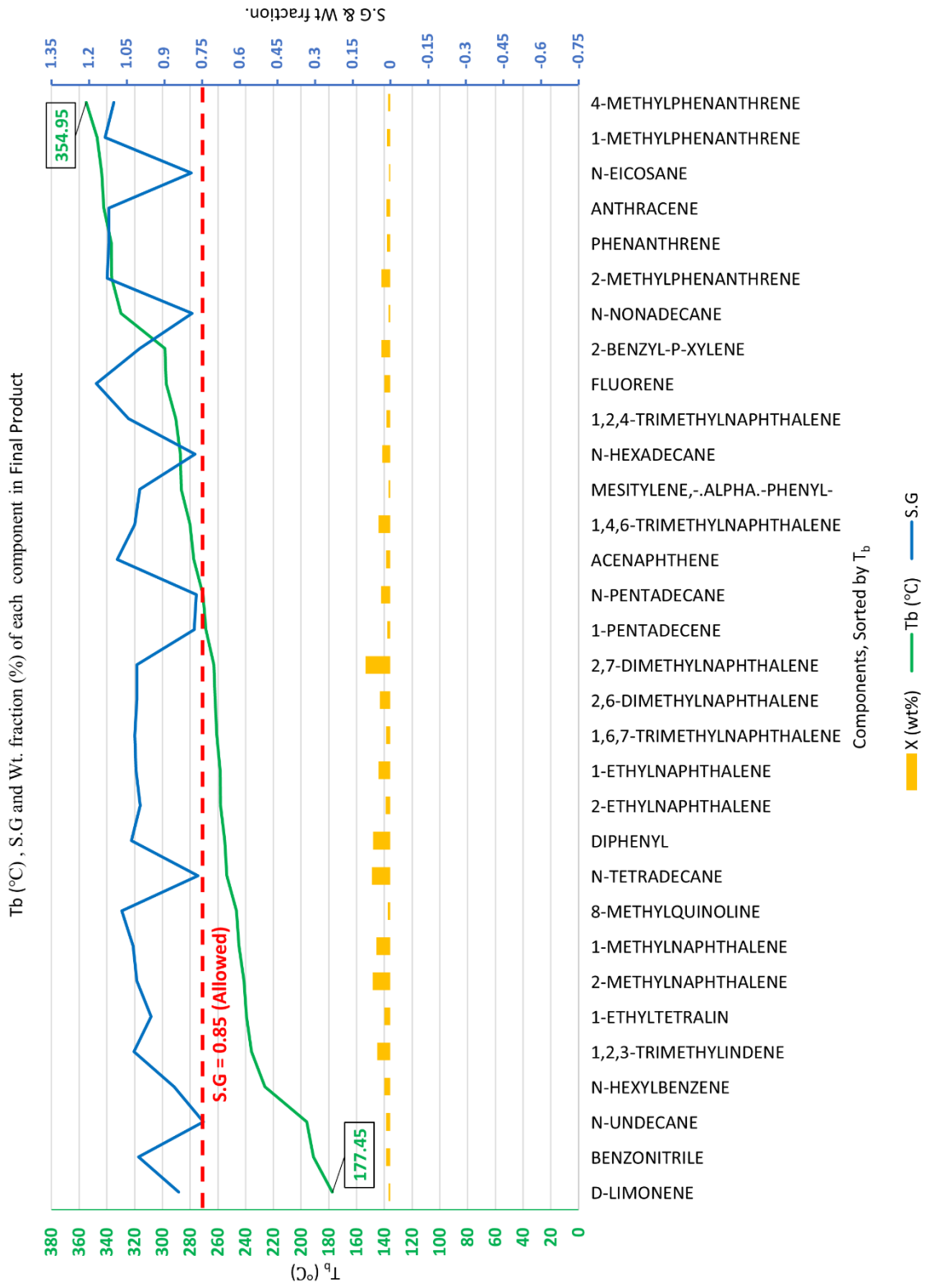


**Fig. 5.** *Components of Final Product and their dencity*

### 7.2. Objective Function

*As mentioned before, the goal of optimizing this process is to increase the yield of pyrolysis diesel production while simultaneously increasing its quality.*

*Therefore, the following parameters have been selected as quantitative and qualitative indicators of diesel for optimization:*

- ***i.*** ***CI:*** *Cetane Index*
- ***ii.*** ***F:*** *Flow Rate*
- ***iii.*** ***SG:*** *Specific Gravity*
- ***iv.*** ***$T_{10}$:*** *Temperature of 10% Recovery as ASTM D86*
- ***v.*** ***$T_{50}$:*** *Temperature of 50% Recovery as ASTM D86.*
- ***vi.*** ***$T_{90}$:*** *Temperature of 90% Recovery as ASTM D86.*

*The first objective function that used is:*

$$O = \frac{F.CI}{(SG - 0.85)(T_{10} - 215)(T_{50} - 260)(T_{90} - 310)}$$

*The denominator parts of the fraction are determined and selected using the Cetane Index calculation formula in the ASTM D4737 standard.*

*But after optimization, we observed that there are some asymptotes, like in T10 = 215 ℃ or T90 = 310 ℃. This causes some apparent and fake optimal points. Also, the the sensitivity of Cetane Index was very low and no useful results were obtained. So the second objective function is developed:*

$$O = \frac{F.CI^2}{(1 + |SG - 0.85|)(1 + |T_{10} - 215|)(1 + |T_{50} - 260|)(1 + |T_{90} - 310|)}$$

*It is evident that the denominator of new objective function has no roots and will not have asymptotes, and the problem of spurious points has been eliminated. Also, the effect of the Cetane index has been increased by a power of 2.*

### 7.3. Optimization Results

*The result was very promising. The parameter values are presented in Table 4. These values were able to satisfy most of the requirements of the mentioned standards to an acceptable extent. However, many changes can still be made to this process to achieve more desirable results.*

**Table 4.** *Results of Objective function parameters:*

| Parameter | Unit | Value |
|---|---|---|
| CI | - | 23.265 |
| F | Kg/hr | 24.225 |
| SG | - | 0.963 |
| $T_{10}$ | ℃ | 242.399 |
| $T_{50}$ | ℃ | 253.458 |
| $T_{90}$ | ℃ | 323.168 |
| O | Kg/hr.(℃)$^3$ | 3.879 |

*Aslo, the results of optimizing variables are presented in Table 5. More data of the simulation is added to Appendix A and B.*

**Table 5.** *Results of Variables*

| Variable | Unit | Value |
|---|---|---|
| $T_R$ | ℃ | 301.8357 |

| | | |
|---|---|---|
| $T_C$ | ℃ | 40 |
| $H_1$ | - | 0.002 |
| $H_2$ | - | 0.1 |
| $L_1$ | - | 0.99 |
| $L_2$ | - | 0.999 |
| $R_1$ | - | 1 |
| $R_2$ | - | 5 |
| $P_{C,1}$ | Bar | 0.2 |
| $P_{C,2}$ | Bar | 0.2 |
| $P_{R,1}$ | Bar | 2 |
| $P_{R,2}$ | Bar | 0.2 |

## *8. EVALUATION OF OPTIMAL CONDITIONS AND RESULTS*

*The successful optimization of the process not only enhanced the quality of the diesel produced but also contributed to a higher overall yield from the pyrolysis of waste tires. These findings underscore the effectiveness of the optimization strategies employed and set the stage for further exploration of the potential applications of the optimized diesel fuel.*

*In conclusion, the optimization process was a systematic and iterative endeavor that involved identifying key parameters, conducting sensitivity analyses, and navigating trade-offs to achieve the desired quality and yield of diesel from waste tire pyrolysis. This phase of the methodology was instrumental in demonstrating the viability of using advanced simulation techniques to enhance renewable energy production from waste materials.*

## *9. LIMITATIONS AND FUTURE WORK*

*While the results of the optimization process are promising, it is essential to acknowledge certain limitations. The simulation model, although validated, may not capture all the complexities of real-world pyrolysis processes, such as variations in feedstock composition and reactor design. Additionally, further experimental validation of the optimized conditions is necessary to confirm the simulation results.*

*Future work could focus on scaling up the process to pilot or industrial levels, where real-time data can be collected and analyzed. Additionally, exploring the integration of other technologies, such as catalytic upgrading or co-processing with other waste materials, could further enhance the quality and yield of the diesel product.*

*In conclusion, the evaluation of results demonstrated the success of the optimization process in producing high-quality diesel fuel from waste tire pyrolysis. The findings highlight the potential of this approach to contribute to sustainable energy solutions while addressing waste management challenges. The insights gained from this study pave the way for further research and development in the field of renewable energy and waste valorization.*

## *10. CONCLUSION*

*The production of high-quality diesel from waste tire pyrolysis not only provides a renewable energy source but also contributes to waste management by reducing the environmental impact of discarded tires. The research undertaken in this study successfully demonstrated the viability of producing diesel fuel from waste tire pyrolysis through an advanced simulation approach. By integrating a detailed pyrolysis model with*

*distillation columns, we were able to optimize the operational parameters to enhance both the yield and quality of the diesel product.*

***APPENDIX A - PARTICLE SIZE DISTRIBUTION (PSD)***

| PSD | Unit | Streams | | |
|---|---|---|---|---|
| | | S1 | S2 | SOLID |
| 0.001-0.002 | m | 0 | 0 | 0 |
| -0.004 | m | 0 | 0 | 0 |
| -0.006 | m | 0 | 0 | 0 |
| -0.008 | m | 0 | 0.2 | 0.2 |
| -0.01 | m | 0 | 0.3 | 0.3 |
| -0.012 | m | 0 | 0.3 | 0.3 |
| -0.015 | m | 0 | 0.2 | 0.2 |
| -0.02 | m | 0 | 0 | 0 |
| -0.05 | m | 0 | 0 | 0 |
| -0.1 | m | 0 | 0 | 0 |
| -0.2 | m | 0 | 0 | 0 |
| -0.3 | m | 0 | 0 | 0 |
| -0.4 | m | 0 | 0 | 0 |
| -0.5 | m | 0 | 0 | 0 |
| -0.6 | m | 0 | 0 | 0 |
| -0.7 | m | 0 | 0 | 0 |
| -0.8 | m | 0 | 0 | 0 |
| -0.9 | m | 0 | 0 | 0 |
| -1 | m | 0 | 0 | 0 |
| -1.1 | m | 0.05 | 0 | 0 |
| -1.2 | m | 0.05 | 0 | 0 |
| -1.3 | m | 0.1 | 0 | 0 |
| -1.4 | m | 0.2 | 0 | 0 |
| -1.5 | m | 0.3 | 0 | 0 |
| -1.6 | m | 0.3 | 0 | 0 |

***APPENDIX B - CONDITIONS OF STREAMS***

| Parameter | Units | Streams | | | | |
|---|---|---|---|---|---|---|
| | | S1 | S2 | S3 | S4 | S5 |
| Temperature | C | 25 | 25 | 300 | 300 | 25 |
| Pressure | bar | 1.01325 | 1.01325 | 1 | 1 | 1 |
| Mass Vapor Fraction | | 0 | 0 | 0.088 | 0.679047 | 0.076657 |
| Mass Density | kg/cum | 1252.994 | 1252.994 | 0.594331 | 3.51844 | 18.15094 |
| Mass Flows | kg/hr | 100 | 100 | 100 | 100.0095 | 67.91114 |

| Parameter | Units | Streams | | | |
|---|---|---|---|---|---|
| | | S6 | S7 | S8 | S9 |
| Temperature | C | 180.7029 | 287.0852 | 3.523382 | 269.7371 |
| Pressure | bar | 0.2 | 0.2 | 1 | 1.5 |
| Mass Vapor Fraction | | 0 | 0 | 0 | 0 |
| Mass Density | kg/cum | 838.4294 | 791.5622 | 823.9429 | 760.1132 |
| Mass Flows | kg/hr | 25.71135 | 3.596947 | 33.39698 | 29.3083 |
| **Parameter** | **Units** | **Streams** | | | |
| | | **G-L** | **GAS** | **LIQUID** | **SOLID** |
| Temperature | C | 300 | 25 | 25 | 300 |
| Pressure | bar | 1 | 1 | 1 | 1 |
| Mass Vapor Fraction | | 1 | 1 | 0 | 0 |
| Mass Density | kg/cum | 2.390208 | 1.418607 | 873.6416 | 2644.559 |
| Mass Flows | kg/hr | 67.91114 | 5.205853 | 62.70529 | 32.09831 |

***APPENDIX C - EQUIPMENT RESULTS***

| Crusher | | RStoic | |
|---|---|---|---|
| Name | *EQ1* | Name | *EQ2* |
| Distribution function | *RRSB* | Specified pressure [bar] | *1* |
| Communition law | *BOND* | Specified temperature [C] | *300* |
| Operating mode | *PRIMARY* | Outlet temperature [C] | *300* |
| Ratio of cut-off size to solids outlet diameter | *1.7* | Outlet pressure [bar] | *1* |
| Open circuit | *NO* | Calculated heat duty [kW] | *44.127* |
| Number of stress events | *1* | Calculated vapor fraction | *1* |
| Interpolation method | *LINEAR* | **RPlug** | |
| Particle diameter > 80% of inlet mass [meter] | *1.533* | Name | *EQ3* |
| Particle diameter > 80% of outlet mass [meter] | *0.012* | Reactor dimensions length [meter] | *1.7* |
| Particle diameter >50% of inlet mass [meter] | *1.433* | Reactor dimensions diameter [meter] | *0.15* |
| Particle diameter > 50% of outlet mass [meter] | *0.01* | Pressure at reactor inlet: process stream [bar] | *0* |
| Size reduction ratio of D80 | *127.778* | Heat duty [kW] | *-10.514* |
| Size reduction ratio of D50 | *143.333* | Minimum reactor temperature [C] | *300* |
| Sauter mean diameter of inlet particles [meter] | *1.389* | Maximum reactor temperature [C] | *300* |
| Sauter mean diameter of outlet particles [meter] | *0.01* | Residence time [sec] | *3.386* |

| Flash2 | | Heater | |
|---|---|---|---|
| Name | EQ6 | Name | EQ5 |
| Temperature [C] | | Specified pressure [bar] | 0 |
| Pressure [bar] | 0 | Specified temperature [C] | 25 |
| Specified heat duty [kW] | 0 | Calculated pressure [bar] | 1 |
| Outlet temperature [C] | 24.979 | Calculated temperature [C] | 25 |
| Outlet pressure [bar] | 1 | Calculated vapor fraction | 0.248 |
| Heat duty [kW] | 0 | Calculated heat duty [kW] | -15.472 |

| Sep | |
|---|---|
| Name | EQ4 |
| Heat duty [kW] | 4.55E-16 |

| DSTWU | | |
|---|---|---|
| Name | EQ7 | EQ8 |
| Reflux ratio | 5 | 5 |
| Light key component recovery | 0.979 | 1 |
| Heavy key component recovery | 0.001 | 0.09 |
| Distillate vapor fraction | 0 | 0 |
| Minimum reflux ratio | 0.299 | 0.036 |
| Actual reflux ratio | 5 | 5 |
| Minimum number of stages | 16.542 | 3.599 |
| Number of actual stage | 17.949 | 3.848 |
| Feed stage | 12.085 | 1.83 |
| Number of actual stage above feed | 11.085 | 0.83 |
| Distillate temperature [C] | 3.525 | 180.703 |
| Bottom temperature [C] | 269.737 | 287.084 |
| Distillate to feed fraction | 0.615 | 0.911 |

***APPENDIX D - REACTIONS AND KINETICS***

| No | Reaction | Product | *A* ($s^{-1}$) | *E* (kJ/mol) | *n* (Temperature coefficient) |
|---|---|---|---|---|---|
| 1 | $C + 2H_2 \rightarrow CH_4$ | Methane | 4.877 | 23.01 | 0 |
| 2 | $2C + 3H_2 \rightarrow C_2H_6$ | Ethane | 0.52 | 23.01 | 0 |
| 3 | $2C + 2H_2 \rightarrow C_2H_4$ | Ethene | 2.386 | 23.01 | 0 |
| 4 | $3C + 4H_2 \rightarrow C_3H_8$ | Propane | 0.277 | 23.01 | 0 |
| 5 | $3C + 3H_2 \rightarrow C_3H_6$ | Propene | 0.446 | 23.01 | 0 |
| 6 | $4C + 5H_2 \rightarrow C_4H_{10}$ | Butane | 0.122 | 23.01 | 0 |
| 7 | $4C + 4H_2 \rightarrow C_4H_8$ | Butene | 0.144 | 23.01 | 0 |
| 8 | $4C + 3H_2 \rightarrow C_4H_6$ | Butalyne | 0.981 | 23.01 | 0 |
| 9 | $C + O_2 \rightarrow CO_2$ | Carbon Dioxide | 0.226 | 23.01 | 0 |

| No | Reaction | Product | *A* ($s^{-1}$) | *E* (kJ/mol) | *n* (Temperature coefficient) |
|---|---|---|---|---|---|
| 10 | $C + {}^{1}O_2 \rightarrow CO$ | Carbon Dioxide | 0.096 | 23.01 | 0 |
| 11 | $H_2 + S \rightarrow H_2S$ | Hydrogen Sulfide | Equilibrium | Equilibrium | 0 |
| 12 | $5C + 6H_2 \rightarrow C_5H_{12}$ | Pentane | 0.339 | 23.01 | 0 |
| 13 | $5C + 4H_2 \rightarrow C_5H_8$ | Pentalyne | 0.066 | 23.01 | 0 |
| 14, 15 | $6C + 6H_2 \rightarrow C_6H_{12}$ | Methylcyclopentene | 0.009, 0.009 | 1.59 | 0 |
| 16 | $8C + 7H_2 \rightarrow C_8H_{14}$ | Methylhexadiene | 0.016 | 1.59 | 0 |
| 17, 19 | $8C + 9H_2 \rightarrow C_8H_{18}$ | Trimethyl-pentane | 0.023, 0.019 | 1.59 | 0 |
| 18 | $7C + 7H_2 \rightarrow C_7H_{14}$ | Dimethyl-cyclopentane | 0.015 | 1.59 | 0 |
| 20 | $8C + 9H_2 \rightarrow C_8H_{18}$ | Dimethylhexane | 0.044 | 1.59 | 0 |
| 21 | $7C + 7H_2 \rightarrow C_7H_{14}$ | Ethylcyclopentane | 0.008 | 1.59 | 0 |
| 22 | $7C + 7H_2 \rightarrow C_7H_{14}$ | Methylcyclohexene | 0.045 | 1.59 | 0 |
| 23 | $8C + 8H_2 \rightarrow C_8H_{16}$ | Dimethyl-cyclohexane | 0.01 | 1.59 | 0 |
| 24 | $8C + 8H_2 \rightarrow C_8H_{16}$ | Octene | 0.007 | 1.59 | 0 |
| 25 | $8C + 7H_2 \rightarrow C_8H_{14}$ | Dimethylhexadiene | 0.011 | 1.59 | 0 |
| 26, 27 | $8C + 8H_2 \rightarrow C_8H_{16}$ | Ethylcyclohexane | 0.054, 0.007 | 1.59 | 0 |
| 28 | $9C + 9H_2 \rightarrow C_9H_{18}$ | Trimethyl-cyclohexane | 0.003 | 1.59 | 0 |
| 29 | $9C + 9H_2 \rightarrow C_9H_{18}$ | Nonene | 0.017 | 1.59 | 0 |
| 30 | $9C + 9H_2 \rightarrow C_9H_{18}$ | Methylocatene | 0.164 | 1.59 | 0 |
| 31 | $10C + 8H_2 \rightarrow C_{10}H_{16}$ | Dlimonene | 0.035 | 1.59 | 0 |
| 32 | $10C + 8H_2 \rightarrow C_{10}H_{16}$ | Pinene | 0.064 | 1.59 | 0 |
| 33 | $10C + 8H_2 \rightarrow C_{10}H_{16}$ | Limonene | 0.619 | 1.59 | 0 |
| 34 | $6C + 3H_2 \rightarrow C_6H_6$ | Benzene | 1.654 | 33.89 | 0 |
| 35 | $7C + 4H_2 \rightarrow C_7H_8$ | Toluene | 7.305 | 33.89 | 0 |
| 36 | $8C + 5H_2 \rightarrow C_8H_{10}$ | Ethylbenzene | 4.708 | 33.89 | 0 |
| 37 | $8C + 5H_2 \rightarrow C_8H_{10}$ | Xylene | 4.476 | 33.89 | 0 |
| 38 | $8C + 4H_2 \rightarrow C_8H_8$ | Styrenetyrene | 4.049 | 33.89 | 0 |
| 39 | $8C + 5H_2 \rightarrow C_8H_{10}$ | Dimethylbenzene | 1.084 | 33.89 | 0 |
| 40 | $9C + 6H_2 \rightarrow C_9H_{12}$ | Cumene | 1.07 | 33.89 | 0 |
| 41 | $9C + 5H_2 \rightarrow C_9H_{10}$ | Ethylmethyl benzene | 0.5 | 33.89 | 0 |
| 42 | $9C + 6H_2 \rightarrow C_9H_{12}$ | Propylbenzene | 1.117 | 33.89 | 0 |
| 43, 44 | $9C + 6H_2 \rightarrow C_9H_{12}$ | Ethylbenzene | 1.189, 2.128 | 33.89 | 0 |
| 45 | $9C + 6H_2 \rightarrow C_9H_{12}$ | Trimethylbenzene | 0.424 | 33.89 | 0 |
| 46 | $6C + 3H_2 + O \rightarrow C_6H_6O$ | Phenol | 0.497 | 33.89 | 0 |

| No | Reaction | Product | $A$ ($s^{-1}$) | $E$ (kJ/mol) | $n$ (Temperature coefficient) |
|---|---|---|---|---|---|
| 47, 51, 52 | $9C + 5H_2 \rightarrow C_9H_{10}$ | Methylethenyl-benzene | 1.532, 0.634, 0.344 | 33.89 | 0 |
| 48 | $7C + 2.5H_2 + N \rightarrow C_7H_5N$ | Benzonitrile | 0.528 | 33.89 | 0 |
| 49 | $9C + 5H_2 \rightarrow C_9H_{10}$ | Propenylbenzene | 0.567 | 33.89 | 0 |
| 50 | $9C + 6H_2 \rightarrow C_9H_{12}$ | $C_3$-benzene | 1.808 | 33.89 | 0 |
| 53 | $10C + 7H_2 \rightarrow C_{10}H_{14}$ | Isopropyltoluene | 3.85 | 33.89 | 0 |
| 54 | $9C + 6H_2 \rightarrow C_9H_{12}$ | $C_3$-benzene | 0.392 | 33.89 | 0 |
| 55 | $9C + 5H_2 \rightarrow C_9H_{10}$ | Dihydro-1H-indene | 0.922 | 33.89 | 0 |
| 56 | $9C + 4H_2 \rightarrow C_9H_8$ | 1H-indene | 1.278 | 33.89 | 0 |
| 57 | $10C + 7H_2 \rightarrow C_{10}H_{14}$ | Butylbenzene | 1.058 | 33.89 | 0 |
| 58 | $10C + 7H_2 \rightarrow C_{10}H_{14}$ | Ethyldimethyl-benzene | 0.338 | 33.89 | 0 |
| 59, 61 | $10C + 7H_2 \rightarrow C_{10}H_{14}$ | Isopropylmethyl-benzene | 0.769, 0.678 | 33.89 | 0 |
| 60 | $10C + 7H_2 \rightarrow C_{10}H_{14}$ | Ethyldimethyl-benzene | 0.397 | 33.89 | 0 |
| 62, 7, 9, 73 | $9C + 5H_2 \rightarrow C_9H_{10}$ | Dihydromethyl-1H-indene | 0.516, 0.759, 3.694, 0.433 | 33.89 | 0 |
| 63 | $10C + 7H_2 \rightarrow C_{10}H_{14}$ | Tetramethylbenzene | 0.383 | 33.89 | 0 |
| 64 | $10C + 7H_2 \rightarrow C_{10}H_{14}$ | Tetramethylbenzene | 0.4 | 33.89 | 0 |
| 65 | $10C + 7H_2 \rightarrow C_{10}H_{14}$ | Ethylisopropyl-benzene | 0.198 | 33.89 | 0 |
| 66 | $8C + 5H_2 + 0.5O_2 \rightarrow C_8H_{10}O$ | Dimethylphenol | 0.316 | 33.89 | 0 |
| 68 | $7C + 3H_2 + O_2 \rightarrow C_7H_6O_2$ | Benzoic acid | 0.549 | 33.89 | 0 |
| 70 | $10C + 5H_2 \rightarrow C_{10}H_{10}$ | Methyl-1H-indene | 0.539 | 33.89 | 0 |
| 71 | $10C + 6H_2 \rightarrow C_{10}H_{12}$ | Tetrahydro-naphalene | 0.562 | 33.89 | 0 |
| 72 | $10C + 7H_2 \rightarrow C_{10}H_{14}$ | $C_4$-benzene | 0.165 | 33.89 | 0 |
| 74 | $10C + 4H_2 \rightarrow C_{10}H_8$ | Naphthalene | 0.979 | 33.89 | 0 |
| 75 | $10C + 7H_2 + 0.5O_2 \rightarrow C_{10}H_{14}O$ | Isopropylphenol | 0.056 | 33.89 | 0 |
| 76 | $7C + 2.5H_2 + 0.5N_2 + 2S \rightarrow C_7H_5NS_2$ | Benzothiazole | 1.2 | 33.89 | 0 |
| 77 | $12C + 8H_2 \rightarrow C_{12}H_{16}$ | Tetrahydro-ethylnaphthalene | 47.264 | 6.3 | -1.089 |
| 78 | $12C + 9H_2 \rightarrow C_{12}H_{18}$ | $C_6$-benzene | 47.815 | 6.3 | -1.089 |
| 79, 80 | $11C + 5H_2 \rightarrow C_{11}H_{10}$ | Methylna-phthalene | 125.001, 156.807 | 6.3 | -1.089 |
| 81, 2 | $12C + 7H_2 \rightarrow C_{12}H_{14}$ | Trimethylindene | 9.307, 95.891 | 6.3 | -1.089 |
| 83 | $12C + 5H_2 \rightarrow C_{12}H_{10}$ | Diphenyl | 142.201 | 6.3 | -1.089 |

| No | Reaction | Product | *A* ($s^{-1}$) | *E* (kJ/mol) | *n* (Temperature coefficient) |
|---|---|---|---|---|---|
| 84, 5 | $12C + 6H_2 \rightarrow C_{12}H_{12}$ | Ethylnaphthalene | 97.289, 37.367 | 6.3 | -1.089 |
| 86, 7, 8 | $12C + 6H_2 \rightarrow C_{12}H_{12}$ | Dimethyl-naphthalene | 85.169, 83.486, 119.843 | 6.3 | -1.089 |
| 89 | $10C + 4.5H_2 + 0.5N_2 \rightarrow C_{10}H_9N$ | Ethylquinoline | 184.356 | 6.3 | -1.089 |
| 90 | $14C + 14H_2 \rightarrow C_{14}H_{28}$ | n-$C_{14}$ | 118.294 | 6.3 | -1.089 |
| 91 | $12C + 5H_2 \rightarrow C_{12}H_{10}$ | Acenaphthene | 36.147 | 6.3 | -1.089 |
| 92 | $15C + 16H_2 \rightarrow C_{15}H_{32}$ | n-$C_{15}$ | 56.974 | 6.3 | -1.089 |
| 93, 4, 5 | $15C + 9H_2 \rightarrow C_{15}H_{18}$ | Trimethyl-naphthalene | 88.852, 31.429, 29.175 | 6.3 | -1.089 |
| 96 | $13C + 5H_2 \rightarrow C_{13}H_{10}$ | Fluorene | 47.77 | 6.3 | -1.089 |
| 97, 8 | $15C + 8H_2 \rightarrow C_{15}H_{16}$ | Dimethyldiphenyl | 60.554, 11.521 | 6.3 | -1.089 |
| 99 | $15C + 15H_2 \rightarrow C_{15}H_{30}$ | Pentadecene | 17.88 | 6.3 | -1.089 |
| 100 | $16C + 17H_2 \rightarrow C_{16}H_{34}$ | n-$C_{16}$ | 46.822 | 6.3 | -1.089 |
| 101 | $14C + 5H_2 \rightarrow C_{14}H_{10}$ | Phenanthrene | 34.666 | 6.3 | -1.089 |
| 102 | $14C + 5H_2 \rightarrow C_{14}H_{10}$ | Anthracene | 38.059 | 6.3 | -1.089 |
| 103 | $15C + 6H_2 \rightarrow C_{15}H_{12}$ | Methyl-phenanthrene | 36.925 | 6.3 | -1.089 |
| 104 | $15C + 15H_2 + O_2 \rightarrow C_{15}H_{30}O_2$ | Pentadecanoic acid | 64.017 | 6.3 | -1.089 |
| 105, 6, 7 | $15C + 6H_2 \rightarrow C_{15}H_{12}$ | Methyl-phenanthrene | 41.028, 46.908, 82.056 | 6.3 | -1.089 |
| 108 | $19C + 20H_2 \rightarrow C_{19}H_{40}$ | n-$C_{19}$ | 12.247 | 6.3 | -1.089 |
| 109 | $19C + 8H_2 \rightarrow C_{19}H_{16}$ | Trimethyl-phenanthrene | 22.599 | 6.3 | -1.089 |
| 110 | $19C + 19H_2 \rightarrow C_{19}H_{38}$ | Isopropyl-methylphenanthrene | 51.627 | 6.3 | -1.089 |
| 111 | $20C + 21H_2 \rightarrow C_{20}H_{42}$ | n-$C_{20}$ | 13.594 | 6.3 | -1.089 |
| 112 | $21C + 22H_2 \rightarrow C_{21}H_{44}$ | n-$C_{21}$ | 15.524 | 6.3 | -1.089 |
| 113 | $22C + 23H_2 \rightarrow C_{22}H_{46}$ | n-$C_{22}$ | 12.028 | 6.3 | -1.089 |
| 114 | $23C + 24H_2 \rightarrow C_{23}H_{48}$ | n-$C_{23}$ | 15.641 | 6.3 | -1.089 |
| 115 | $24C + 25H_2 \rightarrow C_{24}H_{50}$ | n-$C_{24}$ | 3.029 | 6.3 | -1.089 |
| 116 | $11C + 12H_2 \rightarrow C_{11}H_{24}$ | n-$C_{11}$ | 35.684 | 6.3 | -1.089 |

**REFERENCES**

[1] *F. A. Ishola, A. O. Inegbenebor, and F. A. Oyawale, "Thermal Modelling for A Pilot Scale Pyrolytic Furnace for Production of Carbon Black," J. Phys. Conf. Ser., vol. 1378, no. 3, Dec. 2019, doi: 10.1088/1742-6596/1378/3/032089.*

[2] *M. J. Kabir, A. A. Chowdhury, and M. G. Rasul, "Pyrolysis of Municipal Green Waste: A Modelling,*

*Simulation and Experimental Analysis," Energies, vol. 8, no. 8, pp. 7522–7541, Aug. 2015, doi: 10.3390/EN8087522.*

[3] *D. Y. C. Leung and C. L. Wang, "Kinetic modeling of scrap tire pyrolysis," Energy & Fuels, vol. 13, no. 2, pp. 421–427, Mar. 1999, doi: 10.1021/EF980124L.*

[4] *E. Aylón et al., "Waste tyre pyrolysis: modelling of a moving bed reactor.," Waste Manag., vol. 30, no. 12, pp. 2530–2536, Dec. 2010, doi: 10.1016/J.WASMAN.2010.04.018.*

[5] *R. Bi et al., "Simulation and techno-economical analysis on the pyrolysis process of waste tire," Energy, vol. 260, Dec. 2022, doi: 10.1016/J.ENERGY.2022.125039.*

[6] *Y. Cao, A. Taghvaie Nakhjiri, and S. Sarkar, "Modelling and simulation of waste tire pyrolysis process for recovery of energy and production of valuable chemicals (BTEX)," Sci. Rep., vol. 13, no. 1, Dec. 2023, doi: 10.1038/S41598-023-33336-3.*

[7] *H. Y. Ismail, A. Abbas, F. Azizi, and J. Zeaiter, "Pyrolysis of waste tires: A modeling and parameter estimation study using Aspen Plus®.," Waste Manag., vol. 60, pp. 482–493, Feb. 2017, doi: 10.1016/J.WASMAN.2016.10.024.*

[8] *L. Rudniak and P. M. Machniewski, "Modelling and experimental investigation of waste tyre pyrolysis process in a laboratory reactor," Chem. Process Eng., vol. 38, no. 3, pp. 445–454, Sep. 2017, doi: 10.1515/CPE-2017-0034.*

[9] *M. Olazar, G. Lopez, M. Arabiourrutia, G. Elordi, R. Aguado, and J. Bilbao, "Kinetic modelling of tyre pyrolysis in a conical spouted bed reactor," J. Anal. Appl. Pyrolysis, vol. 81, no. 1, pp. 127–132, 2008, doi: 10.1016/J.JAAP.2007.09.011.*

[10] *M. F. Laresgoiti, B. M. Caballero, I. De Marco, A. Torres, M. A. Cabrero, and M. J. Chomón, "Characterization of the liquid products obtained in tyre pyrolysis," J. Anal. Appl. Pyrolysis, vol. 71, no. 2, pp. 917–934, 2004, doi: 10.1016/J.JAAP.2003.12.003.*